Macromolecules

pubs.acs.org/Macromolecules Article

Robust and Programmable Liquid Crystal Elastomers through Catalytic Control of Dynamic Aza-Michael Reactions

Elina Ghimire, Charlie A. Lindberg, Tyler D. Jorgenson, Chuqiao Chen, Juan J. de Pablo, Neil D. Dolinski,* and Stuart J. Rowan*

Cite This: *Macromolecules* 2024, 57, 682−690 Read Online

ACCESS | Metrics & More | Article Recommendations | Supporting Information

ABSTRACT: A strategy to efficiently synthesize thermally reprogrammable but mechanically stable liquid crystalline elastomers (LCEs) is reported by investigating the catalytic effects of para-substituted phenols on dynamic aza-Michael reactions. The synthesis of aza-Michael LCEs was optimized based on a study of catalyzed small-molecule aza-Michael reactions, where the presence of an electron-withdrawing substituent significantly improved the reactivity of the aza-Michael system. The catalysts were then screened to study their effects on the dynamic exchange of aza-Michael adducts. Catalysts with electron-withdrawing substituents were efficient in inducing the dynamic exchange of aza-Michael bonds, thus influencing the mesogen alignment and actuation. After programming the mesogen alignment, the catalyst was washed away to dramatically reduce the dynamic activity and improve the creep resistance of the material while preserving the postsynthetic alignment. This approach represents a straightforward and accessible methodology for efficiently obtaining thermally programmable as well as mechanically stable actuators from dynamic aza-Michael LCEs.

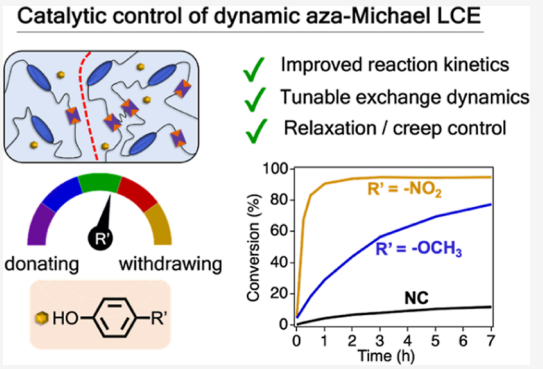

INTRODUCTION

In recent years, soft actuators have garnered attention in healthcare,[1−3] robotics and electronics,[4−6] and manufacturing,[7,8] thanks to their multiresponsive, reversible, and tunable actuation. Liquid crystalline elastomers (LCEs) are ideal candidates for soft actuation applications as they can undergo large reversible dimensional changes, driven by the interplay between the entropic elasticity of the network and the anisotropy of small-molecule liquid crystals.[9−11] LCEs are lightly cross-linked polymer networks with covalently bonded rod-shaped liquid crystalline units (known as mesogens), where the mesogens are typically aligned in a monodomain state to access actuation properties.[12,13] While the monodomain orientation of mesogens is required for actuation purposes, the preferred equilibrium configuration of LCEs during synthesis is a polydomain state (Figure 1a).[14,15] To obtain monodomain LCEs, a range of different techniques have been utilized.[16−18] The two-stage cross-linking method, where a partially cross-linked gel is mechanically stretched to align the mesogens before completely curing the network, was the first technique developed by Küpfer and Finklemann.[19] In recent years, the two-step cross-linking method has been improved through the implementation of click chemistries followed by photo-cross-linking;[20] however, the requirement for UV irradiation for cross-linking introduces additional challenges such as the unintended leaching out of residual photoinitiators and the inhomogeneous curing profile due to the limited penetration depth of light.[21] Other techniques such as surface alignment,[22−24] shear extrusion,[25] and external field-induced alignment[26−28] have also been implemented. However, it can be difficult to obtain mesogen alignment in the bulk of the sample via these techniques, limiting the applications of LCEs to thin films or micron-sized actuators. Moreover, as with any thermoset materials, these techniques generate permanently cross-linked networks that lack reprocessability and recyclability.

Dynamic LCEs, in which the LCE contains dynamic covalent bonds, allow access to networks in which topological rearrangements are possible through dynamic bond exchange, allowing for postsynthetic mesogen alignment (Figure 1b).[17,29−32] As a result, by orienting the mesogen alignment in different directions while concurrently inducing dynamic bond exchange, a variety of actuators can be obtained from the same batch of fully cross-linked LCE networks. Moreover, the actuators can be reprocessed and reshaped into alternating designs. As this method facilitates a facile and robust way to program mesogen alignment via network rearrangement, a

Received: November 12, 2023
Revised: December 22, 2023
Accepted: December 29, 2023
Published: January 9, 2024

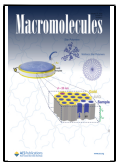

https://doi.org/10.1021/acs.macromol.3c02318
Macromolecules 2024, 57, 682−690

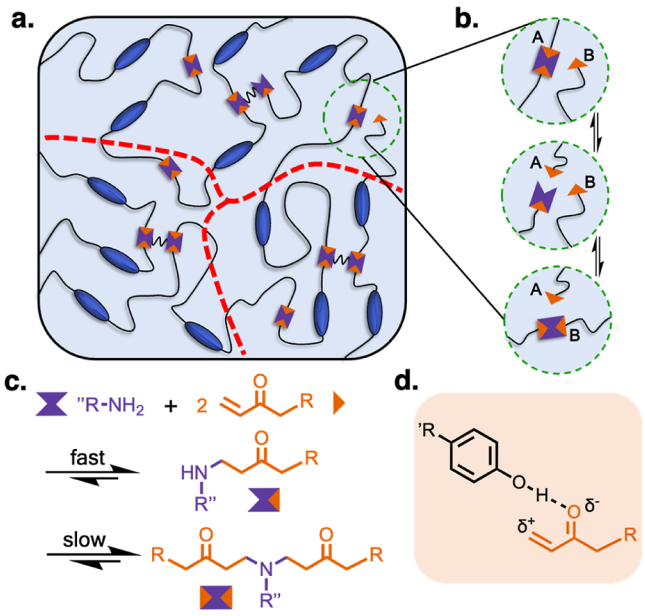

Figure 1. (a) Schematic of the polydomain LCE; (b) scheme showing the dissociative dynamic exchange process; (c) general scheme of the aza-Michael reaction; and (d) interaction of the catalyst with an acrylate.

variety of dynamic chemistries have been explored, which include transesterification,[31,33] disulfide bond exchange,[32,34,35] boronic transesterification,[36] and siloxane exchange.[36,37] It is important to note that there is always a trade-off between ease of thermal reprogrammability and network stability in a dynamic network.[38] The dynamic chemistries that require high thermal energies for activation are difficult to activate without causing side reactions; conversely, those only requiring mild conditions are more susceptible to creep during use.[39] For example, dynamic chemistries such as transesterification and disulfide exchange reactions have high activation energies and are desirable for creep resistance during actuation but require relatively high thermal energies for reprogramming.[31,35] On the other hand, dynamic chemistry such as boronic transesterification, with its low activation energy, allows for facile reprogrammability but can be more susceptible to creep.[39] As a result, circumventing the issue of creep deformation in dynamic LCEs while maintaining the ability to thermally reprogram, reprocess, and remold the networks remains an actively explored challenge in the field.[29,40]

In transesterification-based dynamic LCEs, various catalysts have been added to lower the activation barrier, which again imposes the problem of creep as the energy barrier decreases.[41] It would be desirable to reduce or "turn off" the catalytic effects post-mesogen alignment to ensure mechanical stability in LCEs during actuation. One way to do so would be to imbibe a catalyst to lower the energy barrier of an otherwise stable dynamic network and remove the catalyst after the network has been programmed. Recently, Ji and co-workers reported a variation of this method where they achieved enhanced creep resistance in siloxane-based LCEs by thermally decomposing the imbibed catalyst after dynamically programming the alignment of mesogens.[42] However, this decomposition required high temperatures (150 °C) under stress, introducing the potential for creep to occur in the material. An alternative approach to achieve creep resistance was reported, where a thermally reversible catalyst was used to tune the reprocessability of disulfide-containing polyurethane networks.[43] However, the activation of the catalyst at high temperatures can be problematic in an LCE system, possibly leading to creep during actuation.

Thus, by manipulating the exchange kinetics of a dynamic network, it is possible to controllably enhance and reduce the thermal activity when desired. The aza-Michael bond is a suitable candidate for such a process as it has been shown to be dynamic only under relatively high-temperature conditions (>150 °C) (Figure 1c).[44] Moreover, the aza-Michael reaction is of great interest to the LCE community as it is one of the common methods to synthesize LCE networks using popular, commercially available reactive diacrylate mesogens such as RM82 and RM257.[22,45−47] However, on account of the low reactivity of the formed secondary amine, subsequent photo-cross-linking of terminal acrylates is generally carried out to ensure an adequate gel-fraction. In addition, the presence of unreacted amines can lead to the degradation of mesogens as they tend to react with esters at high temperatures.[21] Therefore, increasing the overall kinetics of the aza-Michael reaction would be useful for LCE synthesis. Recently, chemical species containing hydroxyl groups (−OH) have been shown to enhance the kinetics of aza-Michael reactions.[48−50] Work by Peryton and Avérous proposed a mechanism for this enhancement where the −OH group is able to form a hydrogen bond with the carbonyl of the Michael acceptor, which increases the electrophilicity of the double bond and helps stabilize the transition state (Figure 1d).[49] Using ethanol as a catalyst, the gelation time of an aza-Michael network was shown to decrease by 1.5 times.[49] For aza-Michael-based LCEs, a 1.5 times improvement in the gelation time would still require multiple days for network formation, where the reaction time would ideally be on the order of hours. Aromatic compounds with phenolic −OH groups contain protons with higher acidity compared to their aliphatic counterparts, which makes them more favorable as hydrogen bonding/acid catalysts.[51] Moreover, the electronics of the phenolic compounds can be systematically tuned by introducing electron-donating/-withdrawing substituents on the phenyl ring to control the electronics of the hydrogen-bonding units and tailor the reactivity of the aza-Michael systems.

Reported herein is an investigation of para-substituted phenolic compounds as efficient organocatalysts for the synthesis and augmented dynamic exchange of aza-Michael LCE networks. Specifically, a series of electronically modified phenols were explored as catalysts to tune the electrophilicity of the Michael acceptor and, therefore, control the kinetics of aza-Michael reactions. Furthermore, to access postsynthetic programmability in LCEs via dynamic bond exchange, the effect of the phenolic catalysts on the dynamic exchange behavior of aza-Michael bonds was investigated, and the impact of the catalysts on the alignment and mechanical properties of the LCEs was explored.

RESULTS AND DISCUSSION

Initial work focused on exploring the impact of the electron-donating/-withdrawing groups on the *para*-position of the phenolic catalysts (*p*-**X**) on the aza-Michael reaction, where the specific groups studied were dimethylamino-(*p*-**DMA**), methoxy-(*p*-**OMe**), hydrogen-(*p*-**H**), cyano-(*p*-**CN**), and nitro-(*p*-**NO_2**). As a model reaction, 2 equiv of 2-ethylhexyl acrylate were reacted at 80 °C with 1 equiv of hexylamine (Figure 2a) in the presence of 10 mol % of the different *p*-**X** catalysts

https://doi.org/10.1021/acs.macromol.3c02318
Macromolecules 2024, 57, 682−690

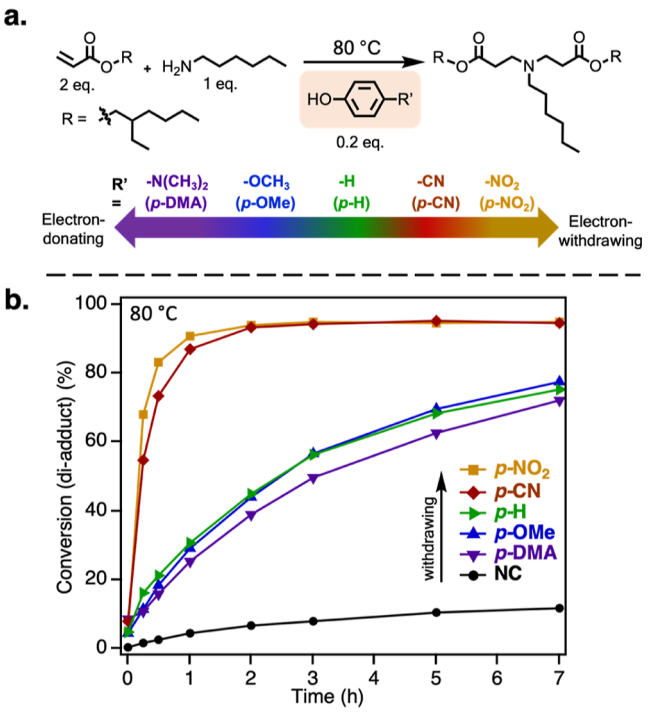

Figure 2. (a) Schematic of the aza-Michael reaction between 2-ethylhexyl acrylate and hexylamine and (b) formation of the diadduct species in the presence of catalysts over time.

(relative to acrylate). During the reaction, the amount of primary (unreacted), secondary (monoadduct), and tertiary (diadduct) amines was monitored via NMR (Figures S1−S7). As was expected based on the existing literature, the initial formation of the monoadduct was relatively fast (Figure S8).[52]

However, as shown in Figure 2b, only about 12% of the reacted products were the diadduct species in the noncatalyzed system (**NC**) after 7 h. The addition of *p*-**H** as a catalyst significantly increased the content of diadduct to about 70−75% in the same time period, suggesting an increased reactivity of the Michael acceptors in the presence of hydrogen bonding species. The electron-donating groups on the *p*-**OMe** and *p*-**DMA** catalysts did not significantly influence the reaction kinetics further and were comparable to the effects of *p*-**H**. However, increasing the electron-withdrawing character of the catalysts (*p*-**CN** and *p*-$\mathbf{NO_2}$) resulted in a significant improvement in the yield of diadduct species (≈94%) within only 3 h. This suggests that the electron-withdrawing groups on *p*-**CN** and *p*-$\mathbf{NO_2}$ further increased the hydrogen-bond donor capability of the phenol, which enhanced the electrophilicity of the acrylates. This understanding can be leveraged to improve the gelation kinetics of aza-Michael-based LCEs as well as other aza-Michael network systems.

To expand the small-molecule studies into the network systems, two catalysts, one with an electron-donating group (*p*-**OMe**) and one with an electron-withdrawing group (*p*-$\mathbf{NO_2}$), were selected to monitor the gelation kinetics of the aza-Michael LCEs. As shown in Figure 3a,b, the LCE networks were composed of the commercially available diacrylate LC monomer (RM82), diamine cross-linker (HMDA), and an amine chain extender (HA). The polymerization was monitored, using shear rheology, at 80 °C in the presence of *p*-**OMe** and *p*-$\mathbf{NO_2}$ catalysts (10 mol % relative to the LC monomer) and compared against the noncatalyzed system.

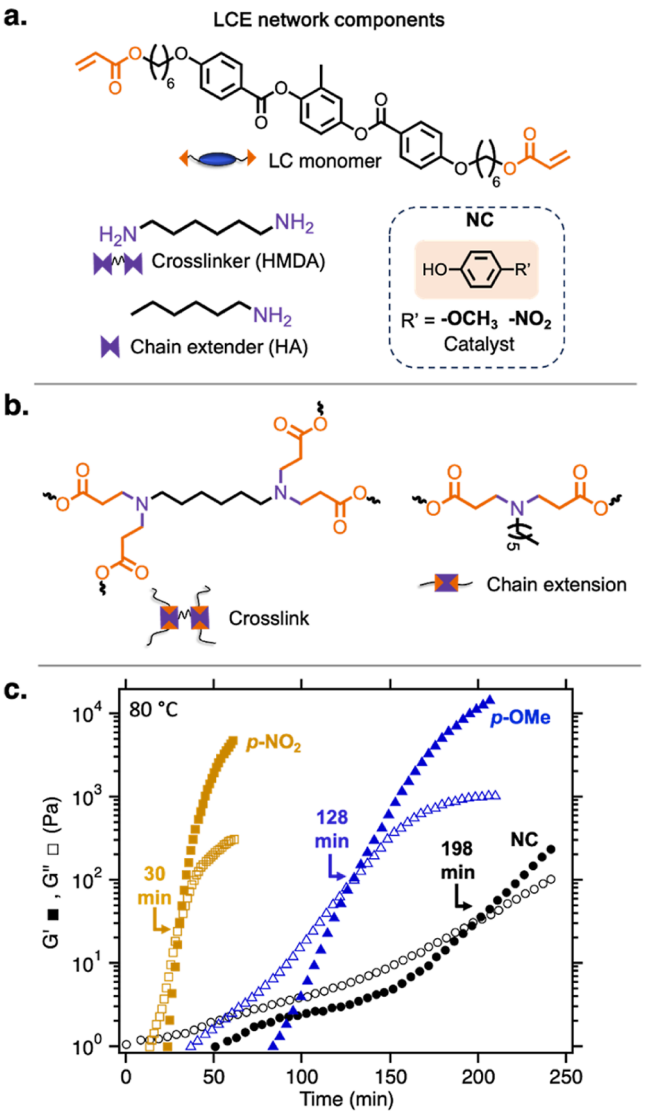

Figure 3. (a) Chemical structures of the LCE network components; (b) schematic illustration of the aza-Michael cross-link and chain-extension in the LCE network; and (c) influence of catalysts on the gelation times of LCEs (small amplitude oscillatory shear rheology, frequency = 1 Hz, parallel plate geometry, 80 °C, and 5% strain).

The gel points, t_{gel}, were determined as the times at which the storage modulus and loss modulus curves crossed over. As shown in Figure 3c, the noncatalyzed system gelled in 198 min, which was decreased to 128 min (1.5 times faster gelation) in *p*-**OMe**-catalyzed and to 30 min (6.6 times faster gelation) in *p*-$\mathbf{NO_2}$-catalyzed systems. The reaction kinetics and the gelation times of the systems containing *p*-$\mathbf{NO_2}$ (Figures 2 and 3) reveal it to be an efficient catalyst for the generation of aza-Michael networks with high gel fractions in relatively short periods of time.

In the absence of a catalyst, the time required to synthesize a fully cured aza-Michael network with good mechanical properties has been reported to be as high as 72 h at 70 °C.[44] Informed by the results in Figure 3c, a catalytic amount of *p*-$\mathbf{NO_2}$ was added to facilitate the synthesis of a fully cured aza-Michael-based LCE network with a theoretical molecular weight of 2000 g/mol between the cross-links. The reaction was carried out at 80 °C for 16 h, which resulted in an LCE with a high gel content (≈94%).

https://doi.org/10.1021/acs.macromol.3c02318
Macromolecules 2024, 57, 682−690

As the phenolic catalysts have been found to enhance the kinetics of the aza-Michael reaction, it was interesting to explore if the catalysts would also influence the dynamic exchange rates of the aza-Michael adducts. Thus, initial studies were focused on the dissociative exchange behavior between two small-molecule aza-Michael adducts. First, two aza-Michael diadduct species were synthesized by reacting 1 equiv of hexylamine with 2 equiv of either ethylhexyl acrylate (**E−N−E**) or benzyl acrylate (**B−N−B**). The two adducts were added together in a 1:1 molar ratio (Figure 4a) in the

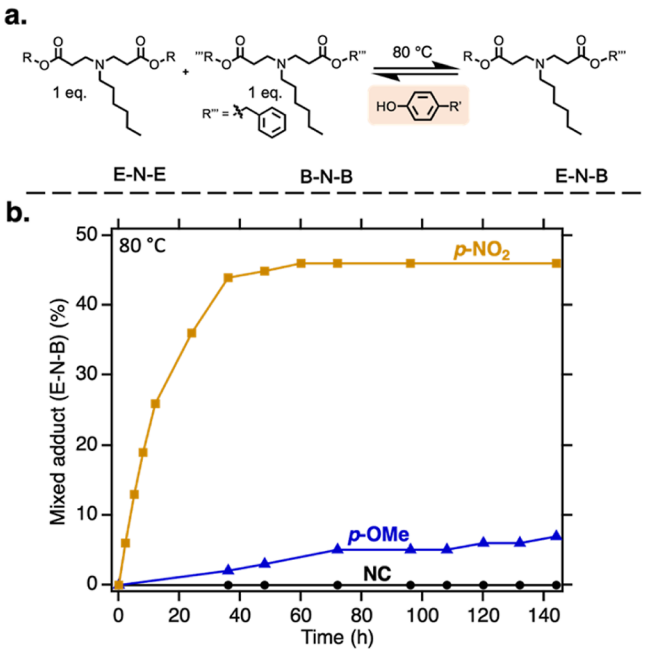

Figure 4. (a) Chemical structures of the aza-Michael adducts used for dynamic exchange kinetics and (b) influence of catalysts in the dynamic exchange of the aza-Michael adducts.

presence of *p*-**NO$_2$** or *p*-**OMe** catalyst or without any catalyst (**NC**) and were monitored at 80 °C for 144 h following the appearance of the ^{1}H NMR signal that belongs to the **E−N−B** (mixed adduct) species (Figure S9). The exchange kinetics of the adducts with and without the catalysts are shown in Figure 4b (for full NMR spectra, see Supporting Information Figures S10−S12). The signals corresponding to **E−N−B** were almost nonexistent in the noncatalyzed system. The *p*-**OMe**- and *p*-**NO$_2$**-catalyzed systems showed observable formation of **E−N−B**, with the latter system reaching an equilibrium point with about 45% of the **E−N−B** adduct after 36 h.

As hypothesized, the phenolic catalysts indeed contributed to the dynamic exchange kinetics of aza-Michael adducts, which were further enhanced by the electron-withdrawing character of the substituent. Compared to previously reported results (requiring significantly higher temperatures (>150 °C) to induce dynamic exchange),[44] aza-Michael exchange reactions can be performed under milder conditions by simply adding *p*-**NO$_2$** as a catalyst. This result provides the opportunity to tailor the dynamic behavior of aza-Michael exchange reactions. For LCE-based films, this potentially allows aza-Michael chemistry to be amenable for both polymerizing the LCE network and programming mesogen alignment without the installation of an additional dynamic bond.

To demonstrate this, the influence of the *p*-**OMe** and *p*-**NO$_2$** catalysts on the dynamic exchange behavior of aza-Michael LCEs was studied. To circumvent any discrepancies in the cross-linking densities of the networks due to the variance in the rates of the aza-Michael reaction with different catalysts, the initial curing was carried out using *p*-**NO$_2$**, which was thoroughly washed out in acetone via Soxhlet extraction. The network was then dried overnight under a vacuum at 60 °C. The successful removal of the catalyst was confirmed by comparing the presence and absence of a peak at 1380 cm^{-1}, corresponding to the NO_2 stretch in infrared spectroscopy, in the as-synthesized and washed systems, respectively (Figure S13). Upon confirming the removal of the catalyst, the as-pressed films (**LCE**) were imbibed with either *p*-**OMe** or *p*-**NO$_2$** via swelling in acetone (Figure 5a), forming **LCE-OMe** and **LCE-NO$_2$**, respectively. Postswelling, the concentration of

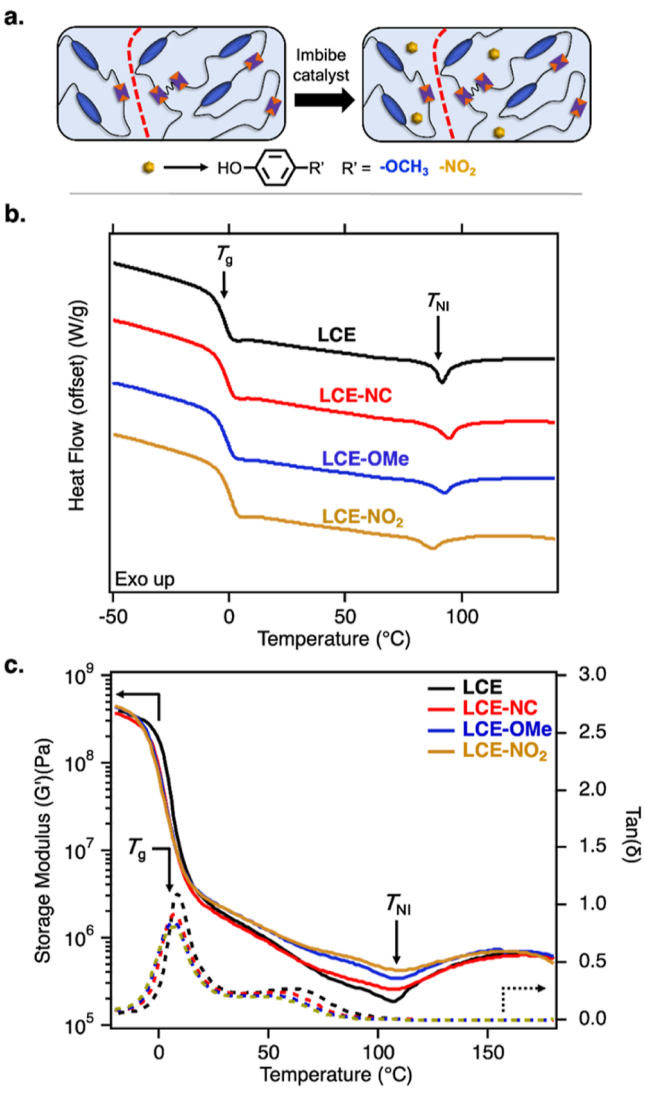

Figure 5. (a) Schematic illustration showing the imbibing of the catalyst into LCEs; (b) differential scanning calorimetry thermograms; and (c) shear rheology dynamic temperature sweeps (temperature ramp rate = 3 °C/min, frequency = 1 Hz, and parallel plate geometry) showing storage moduli (solid lines) and tan delta (dashed lines) of the LCEs with no catalyst (**LCE-NC**) and those imbibed with either *p*-methoxyphenol (**LCE-OMe**) or *p*-nitrophenol (**LCE-NO$_2$**).

https://doi.org/10.1021/acs.macromol.3c02318
Macromolecules 2024, 57, 682−690

the catalyst remaining in the solution was used to calculate the amount of catalyst that was imbibed into the films, which was ∼2 mol % relative to the diacrylate LC mesogen. Once the films were completely swollen, they were vacuum-dried before further studies. To separate any potential influence of the swelling process on material properties, a control sample was made where an LCE film without any catalyst was swollen and subsequently dried (**LCE-NC**). The removal of the solvent for all three samples was confirmed by thermogravimetric analysis (Figure S14).

The thermal transition temperatures were measured using differential scanning calorimetry. The glass transition temperatures (T_g) of all four systems were very similar (between 0 and −3 °C), and the nematic to isotropic transition temperatures (T_{NI}) were within the range of 91 ± 4 °C (Figure 5b), demonstrating that the thermal transitions of the LCEs were not significantly impacted by the imbibing procedure. In addition, the thermomechanical behavior of the networks was studied by conducting dynamic temperature ramp measurements using shear rheology. The G' curves in Figure 5c illustrate that all four systems display comparable storage moduli across the entire temperature range probed (−20 to 180 °C). The temporary decrease in storage moduli curves occurring around T_{NI} indicates the presence of dynamic soft elasticity in the LCEs.[53] For all materials studied, the storage moduli after the T_{NI} increased, and the LCEs behaved like amorphous rubbery networks beyond the clearing temperature.[53] Typical to LCEs, two peaks were observed in tan δ, where the first peak corresponds to the T_g of the material and the second peak arises from the combined energy dissipation resulting from domain rotation and the viscous deformation of non-LC segments.[53] The nonlinear tensile properties of these materials were also similar to one another, as evidenced by the stress−strain response obtained from tensile test measurements (Figure S15). These observations confirm the minimal effect of the catalyst imbibing procedure on the thermomechanical and liquid-crystalline properties of the materials.

To understand the influence of phenolic catalysts on the dynamic exchange behavior of the aza-Michael LCEs, shear stress relaxation studies were conducted. To decouple the contribution of domain rotation in stress relaxation, the measurements were conducted above the T_{NI} of the LCEs. The aza-Michael LCEs indeed behave as thermally induced dynamic networks, as evidenced by the temperature-dependent stress relaxation shown in Figures S16−S18.

Characteristic relaxation times (τ^*) were obtained by fitting the relaxation data to a stretched exponential function. The τ^* values were then plotted as a function of temperature and took the form of an Arrhenius relationship from which activation energies (E_a) and Arrhenius prefactor (τ_0) values were obtained. The effects of ***p*-OMe** and ***p*-NO$_2$** catalysts are clearly observed in the dynamic exchange rates of LCEs, as shown in Figure 6a, where the relaxation times of the catalyzed systems at 160 °C are shorter than that of **LCE-NC**. The stress relaxation in **LCE-NC** is observed as the retro-aza-Michael reaction, which is known to occur at such temperatures,[44] and is accelerated in **LCE-OMe** and **LCE-NO$_2$** due to the presence of catalysts. As shown in Figure 6b, the E_a values calculated for all three systems were within error of each other. However, the absolute kinetics of the reactions were affected by the catalysts, resulting in differences in the rates of stress relaxation. On average, the τ^* value for **LCE-NC** was 1250 s, which decreased

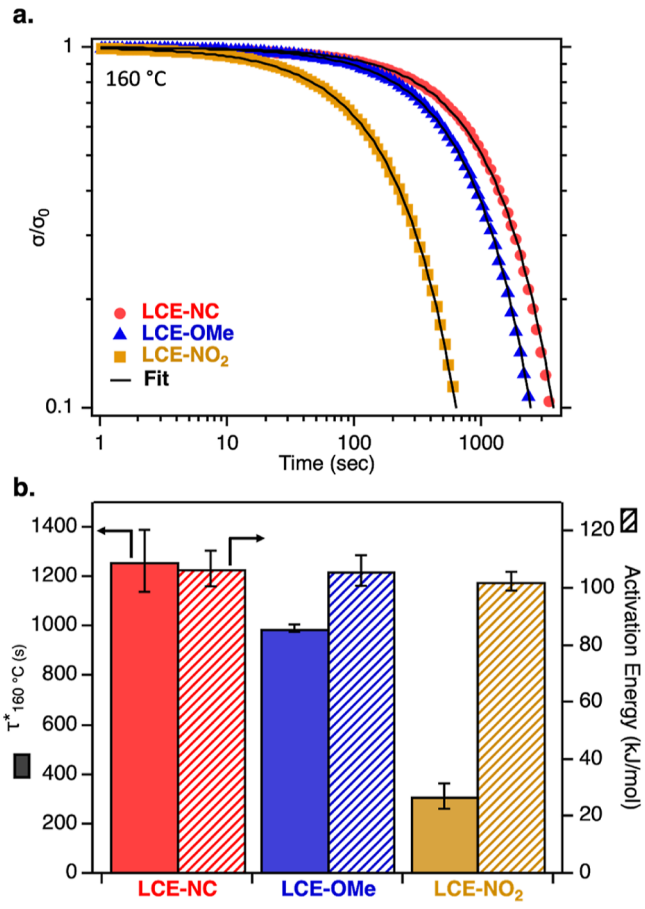

Figure 6. Comparison of the stress relaxation behavior of the LCE with no catalyst (**LCE-NC**) and those imbibed with either *p*-methoxyphenol (**LCE-OMe**) or *p*-nitrophenol (**LCE-NO$_2$**). (a) Normalized stress relaxation data at 160 °C with stretched exponential fits (solid black lines) (temperature ramp rate = 3 °C/min, frequency = 1 Hz, and parallel plate geometry) and (b) characteristic relaxation times at 160 °C (error bars are based on standard deviations from three measurements) and calculated activation energy values (error bars are based on the error propagation of the fits).

to 1000 s in **LCE-OMe** and to 300 s in **LCE-NO$_2$**. Through the selection of catalysts, the time scales necessary for the dynamic reprogramming of aza-Michael LCEs can be directly manipulated, therefore imparting control over the programming of mesogen alignment in LCEs.

The schematic for programming the mesogen alignment is shown in Figure 7a. First, **LCE-NC**, **LCE-OMe**, and **LCE-NO$_2$** were stretched from their polydomain to monodomain states to align the mesogens in a uniaxial direction. The stretched monodomain LCEs were placed between two glass slides and held together by binder clips, which were then allowed to undergo stress relaxation at 80 °C for 15 h, resulting in relaxed monodomain states.

To quantify the alignment of mesogens, wide-angle X-ray scattering (WAXS) measurements were performed. The 2D patterns for the three material systems are shown in Figure 7b, where the top and bottom rows represent the samples before and after programming, respectively. Before programming, all three systems exhibit uniform 2D patterns, suggesting a lack of preferred directionality in the mesogen orientation. After programming, **LCE-NC** continues to exhibit an isotropic ring,

https://doi.org/10.1021/acs.macromol.3c02318
Macromolecules 2024, 57, 682−690

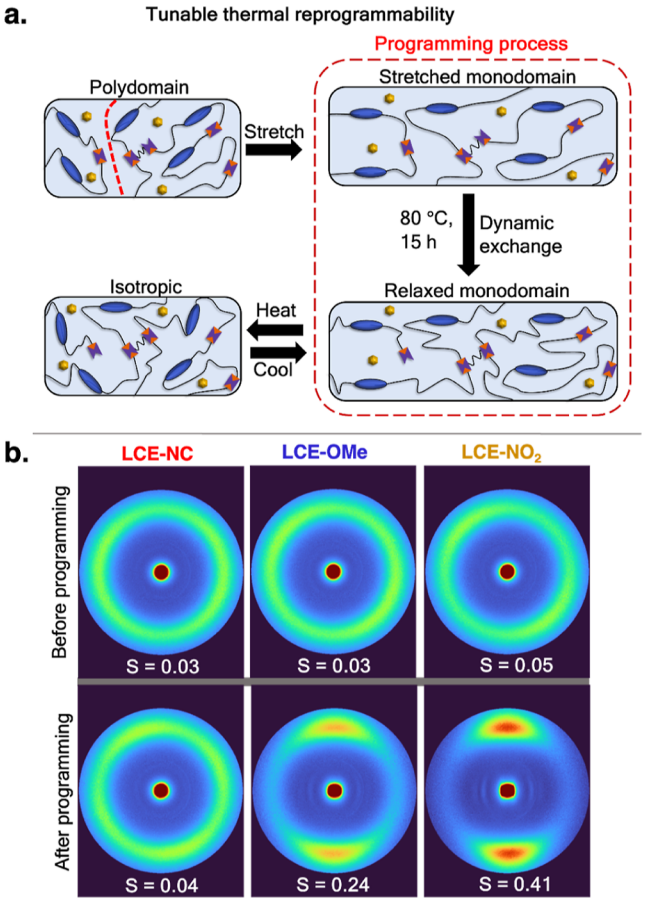

Figure 7. (a) Schematic illustration showing the programming procedure in dynamic LCEs. (b) WAXS images of the LCEs with no catalyst (**LCE-NC**) and those imbibed with either *p*-methoxyphenol (**LCE-OMe**) or *p*-nitrophenol (**LCE-NO$_2$**) before and after programming.

similar to its nonprogrammed counterpart. On the other hand, the 2D patterns of **LCE-OMe** and **LCE-NO$_2$** after programming show increased intensities on their vertical axes, suggesting the preferential orientation of mesogens in the horizontal direction (parallel to the direction of the strain applied during the programming procedure). The intensities of the WAXS images were plotted as a function of azimuthal angle (Figure S20), from which order parameters (S) were calculated based on the Kratky method.[54] The S values are expected to fall between 0 and 1, with an isotropic sample approaching a value of $S = 0$ and an aligned sample approaching a value of $S = 1$.

As shown in Figure 7b, **LCE-NC** showed no significant change in the order parameter. However, both LCEs with catalysts (**LCE-OMe** and **LCE-NO$_2$**) exhibit higher-order parameters after programming, with **LCE-NO$_2$** having the largest change. This suggests that the alignment of mesogens was more effective in **LCE-NO$_2$**, presumably as a result of the faster relaxation kinetics enabled by the *p*-**NO$_2$** catalyst during the programming process. In addition, the effect of mesogen alignment was observed in the actuation strains of the samples, which were calculated based on their relaxed lengths at room temperature and their contracted lengths above the T_{NI}. As shown in Figure S21, **LCE-NO$_2$** exhibited the highest actuation, with an average of 31%. On the other hand, **LCE-NC** and **LCE-OMe** showed minimal actuation. Moreover, after programming, **LCE-NO$_2$** did not exhibit a soft elastic region when stretched in the direction parallel to the orientation of mesogens, suggesting a uniaxial alignment of mesogens (Figure S22). In addition, the orientation of mesogens was monitored using polarized optical microscopy (POM), where **LCE-NO$_2$** exhibited uniaxial alignment of mesogens after programming (Figure S23). The data highlight the ability to control the thermal reprogrammability of LCEs by incorporating catalysts that impact the reaction kinetics of the aza-Michael bond exchange.

While the enhanced dynamic exchange kinetics of the **LCE-NO$_2$** system is useful for shape reprogramming, it is more prone toward creep deformation. Particularly, as the LCEs are thermally cycled to access their actuation properties, the fast reaction kinetics of the aza-Michael bonds in **LCE-NO$_2$** can

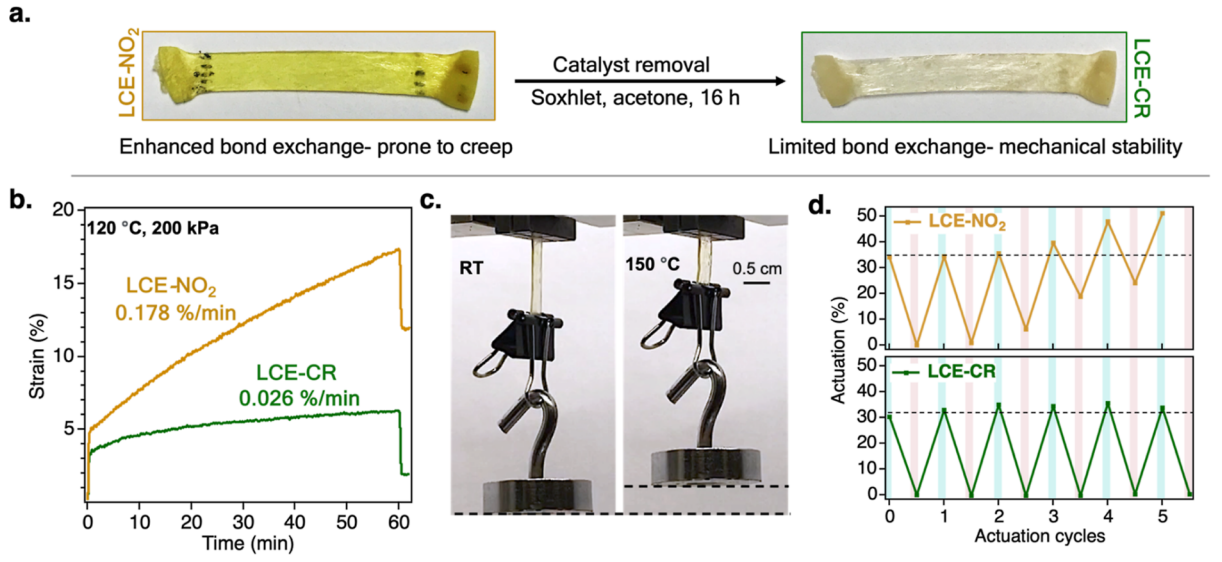

Figure 8. (a) Images of LCEs before and after the removal of the catalyst; (b) creep measurements of LCEs before and after the removal of the catalyst; (c) images of **LCE-CR** during actuation; and (d) actuation cycles of **LCE-NO$_2$** (top) and **LCE-CR** (bottom) between 20 and 150 °C, the **LCE-NO$_2$** sample failed after 5 actuation cycles (teal = 20 °C and pink = 150 °C).

https://doi.org/10.1021/acs.macromol.3c02318
Macromolecules 2024, 57, 682−690

lead to undesirable levels of reactivity, thus affecting the network stability. Therefore, to inhibit the reactivity of aza-Michael bonds postprogramming, the programmed **LCE-NO$_2$** film was swollen in acetone to selectively remove the *p*-**NO$_2$** catalyst, forming **LCE-CR** (Figure 8a). The thermal stabilities of **LCE-NO$_2$** and **LCE-CR** were compared by performing creep measurements, which were conducted by the application of 200 kPa load for 1 h at 120 °C. The measurements were conducted above the T_{NI} to prevent any possible impact on dimensional change due to the rotation of mesogens during the nematic to isotropic transition. As shown in Figure 8b, the rate of creep deformation was reduced by more than seven times by suppressing the catalytically enhanced thermal activation of the aza-Michael bonds. In addition, the actuation performances of **LCE-NO$_2$** and **LCE-CR** were compared. Figure 8c shows the images of **LCE-CR** during elongation and contraction at room temperature and 150 °C, respectively. Repeated actuation cycles were performed using dynamic mechanical analysis, where the samples were heated and cooled between 150 and 20 °C with a constant load of 0.15 N. Unlike the common practice of performing actuation cycles in load-free states, here we applied a constant load throughout the measurement to better compare their performance during application conditions. Compared to **LCE-NO$_2$**, **LCE-CR** exhibited drastically improved network stability without losing its actuation capability, as shown in Figure 8b,d.

CONCLUSIONS

In this work, a series of phenolic catalysts with different electronic characteristics were studied in the formation and dissociation of aza-Michael adducts. A hydrogen bonding catalyst with an electron-withdrawing group (*p*-**NO$_2$**) was used to optimize the synthesis of aza-Michael LCEs. By tuning the exchange rates of the aza-Michael bonds with different catalysts, the reprogrammability of the mesogen alignment in the LCEs was systematically controlled. Moreover, the mechanical stability of the programmed LCE could be maintained by removing the catalyst postprogramming. The insights from this project will be useful in the future utilization of aza-Michael chemistry to synthesize programmable and mechanically stable dynamic LCEs.

ASSOCIATED CONTENT

Supporting Information

The Supporting Information is available free of charge at https://pubs.acs.org/doi/10.1021/acs.macromol.3c02318.

^{1}H NMR spectra for all kinetics experiments, additional experimental details, materials and methods, including photographs of samples, thermo-mechanical characterizations, IR spectroscopy measurements, isostress measurements, 1D WAXS profiles, POM images, and actuation cycles (PDF)

AUTHOR INFORMATION

Corresponding Authors

Neil D. Dolinski − *Pritzker School of Molecular Engineering, University of Chicago, Chicago, Illinois 60637, United States;* Present Address: Department of Chemical Engineering, Columbia University, New York, NY 10027, United States; orcid.org/0000-0002-2160-8811; Email: nd2827@columbia.edu

Stuart J. Rowan − *Pritzker School of Molecular Engineering, University of Chicago, Chicago, Illinois 60637, United States; Center for Molecular Engineering, Argonne National Laboratory, Lemont, Illinois 60434, United States; Department of Chemistry, University of Chicago, Chicago, Illinois 60637, United States;* orcid.org/0000-0001-8176-0594; Email: stuartrowan@uchicago.edu

Authors

Elina Ghimire − *Pritzker School of Molecular Engineering, University of Chicago, Chicago, Illinois 60637, United States*

Charlie A. Lindberg − *Pritzker School of Molecular Engineering, University of Chicago, Chicago, Illinois 60637, United States*

Tyler D. Jorgenson − *Pritzker School of Molecular Engineering, University of Chicago, Chicago, Illinois 60637, United States*

Chuqiao Chen − *Pritzker School of Molecular Engineering, University of Chicago, Chicago, Illinois 60637, United States;* orcid.org/0000-0002-4844-5098

Juan J. de Pablo − *Pritzker School of Molecular Engineering, University of Chicago, Chicago, Illinois 60637, United States; Center for Molecular Engineering, Argonne National Laboratory, Lemont, Illinois 60434, United States;* orcid.org/0000-0002-3526-516X

Complete contact information is available at: https://pubs.acs.org/10.1021/acs.macromol.3c02318

Author Contributions

E.G. performed the experiments and analyzed the results. T.D.J. collected the data for the gel point measurement study. C.C. worked up and plotted the data for WAXS measurements. E.G. wrote the manuscript. C.A.L., T.D.J., C.C., N.D.D., and S.J.R. edited the manuscript. E.G. and C.A.L. conceptualized the research idea. N.D.D. and S.J.R. supervised the project. J.J.d. P. and S.J.R. provided financial support for the project.

Notes

The authors declare no competing financial interest.

ACKNOWLEDGMENTS

This work was primarily supported by the University of Chicago Materials Research Science and Engineering Center, which is funded by the National Science Foundation under award number DMR-2011854. C.C. was supported by a University of Chicago MRSEC Fellowship under award number DMR-2011854. Parts of this work were carried out at the Soft Matter Characterization Facility and at the Materials Research Science and Engineering Center at the University of Chicago.

REFERENCES

(1) Roche, E. T.; Horvath, M. A.; Wamala, I.; Alazmani, A.; Song, S. E.; Whyte, W.; Machaidze, Z.; Payne, C. J.; Weaver, J. C.; Fishbein, G.; Kuebler, J.; Vasilyev, N. V.; Mooney, D. J.; Pigula, F. A.; Walsh, C. J. Soft Robotic Sleeve Supports Heart Function. *Sci. Transl. Med.* **2017**, *9*, No. eaaf3925.

(2) Agarwal, G.; Besuchet, N.; Audergon, B.; Paik, J. Stretchable Materials for Robust Soft Actuators towards Assistive Wearable Devices. *Sci. Rep.* **2016**, *6*, 34224.

(3) Shaha, R. K.; Merkel, D. R.; Anderson, M. P.; Devereaux, E. J.; Patel, R. R.; Torbati, A. H.; Willett, N.; Yakacki, C. M.; Frick, C. P. Biocompatible Liquid-Crystal Elastomers Mimic the Intervertebral Disc. *J. Mech. Behav. Biomed. Mater.* **2020**, *107*, 103757.

(4) Cacucciolo, V.; Shintake, J.; Kuwajima, Y.; Maeda, S.; Floreano, D.; Shea, H. Stretchable Pumps for Soft Machines. *Nature* **2019**, *572* (7770), 516−519.
(5) Mishra, A. K.; Del Dottore, E.; Sadeghi, A.; Mondini, A.; Mazzolai, B. SIMBA: Tendon-Driven Modular Continuum Arm with Soft Reconfigurable Gripper. *Front. Robot.* **2017**, *4*, 4.
(6) Aksoy, B.; Shea, H. Reconfigurable and Latchable Shape-Morphing Dielectric Elastomers Based on Local Stiffness Modulation. *Adv. Funct. Mater.* **2020**, *30*, 2001597.
(7) Tolley, M. T.; Shepherd, R. F.; Mosadegh, B.; Galloway, K. C.; Wehner, M.; Karpelson, M.; Wood, R. J.; Whitesides, G. M. A Resilient, Untethered Soft Robot. *Soft Robot.* **2014**, *1* (3), 213−223.
(8) Kang, D. J.; An, S.; Yarin, A. L.; Anand, S. Programmable Soft Robotics Based on Nano-Textured Thermo-Responsive Actuators. *Nanoscale* **2019**, *11* (4), 2065−2070.
(9) White, T. J.; Broer, D. J. Programmable and Adaptive Mechanics with Liquid Crystal Polymer Networks and Elastomers. *Nat. Mater.* **2015**, *14* (11), 1087−1098.
(10) Ohm, C.; Brehmer, M.; Zentel, R. Liquid Crystalline Elastomers as Actuators and Sensors. *Adv. Mater.* **2010**, *22* (31), 3366−3387.
(11) Kularatne, R. S.; Kim, H.; Boothby, J. M.; Ware, T. H. Liquid Crystal Elastomer Actuators: Synthesis, Alignment, and Applications. *J. Polym. Sci., Part B: Polym. Phys.* **2017**, *55*, 395−411.
(12) Yu, Y.; Ikeda, T. Soft Actuators Based on Liquid-Crystalline Elastomers. *Angew. Chem., Int. Ed.* **2006**, *45* (33), 5416−5418.
(13) Warner, M.; Terentjev, E. M. *Liquid Crystal Elastomers*; Oxford University Press, 2007; Vol. *120*.
(14) Petridis, L.; Terentjev, E. M. Nematic-Isotropic Transition with Quenched Disorder. *Phys. Rev. E: Stat., Nonlinear, Soft Matter Phys.* **2006**, *74* (5), 051707.
(15) Clarke, S. M.; Nishikawa, E.; Finkelmann, H.; Terentjev, E. M. Light-Scattering Study of Random Disorder in Liquid Crystalline Elastomers. *Macromol. Chem. Phys.* **1997**, *198* (11), 3485−3498.
(16) Herbert, K. M.; Fowler, H. E.; McCracken, J. M.; Schlafmann, K. R.; Koch, J. A.; White, T. J. Synthesis and Alignment of Liquid Crystalline Elastomers. *Nat. Rev. Mater.* **2021**, *7*, 23−38.
(17) Saed, M. O.; Gablier, A.; Terentjev, E. M. Exchangeable Liquid Crystalline Elastomers and Their Applications. *Chem. Rev.* **2022**, *122* (5), 4927−4945.
(18) Ula, S. W.; Traugutt, N. A.; Volpe, R. H.; Patel, R. R.; Yu, K.; Yakacki, C. M. Liquid Crystal Elastomers: An Introduction and Review of Emerging Technologies. *Liq. Cryst. Rev.* **2018**, *6*, 78−107.
(19) Küpfer, J.; Finkelmann, H. Nematic Liquid Single Crystal Elastomers. *Makromol. Chem., Rapid Commun.* **1991**, *12*, 717−726.
(20) Yakacki, C. M.; Saed, M.; Nair, D. P.; Gong, T.; Reed, S. M.; Bowman, C. N. Tailorable and Programmable Liquid-Crystalline Elastomers Using a Two-Stage Thiol-Acrylate Reaction. *RSC Adv.* **2015**, *5* (25), 18997−19001.
(21) Zou, W.; Lin, X.; Terentjev, E. M. Amine-Acrylate Liquid Single Crystal Elastomers Reinforced by Hydrogen Bonding. *Adv. Mater.* **2021**, *33* (30), 2101955.
(22) Ware, T. H.; McConney, M. E.; Wie, J. J.; Tondiglia, V. P.; White, T. J. Voxelated Liquid Crystal Elastomers. *Science* **2015**, *347* (6225), 982−984.
(23) McCracken, J. M.; Hoang, J. D.; Herman, J. A.; Lynch, K. M.; White, T. J. Millimeter-Thick Liquid Crystalline Elastomer Actuators Prepared by-Surface-Enforced Alignment. *Adv. Mater. Technol.* **2023**, *8* (13), 2202067.
(24) Hebner, T. S.; Kirkpatrick, B. E.; Anseth, K. S.; Bowman, C. N.; White, T. J. Surface-Enforced Alignment of Reprogrammable Liquid Crystalline Elastomers. *Advanced Science* **2022**, *9* (29), 2204003.
(25) Ambulo, C. P.; Burroughs, J. J.; Boothby, J. M.; Kim, H.; Shankar, M. R.; Ware, T. H. Four-Dimensional Printing of Liquid Crystal Elastomers. *ACS Appl. Mater. Interfaces* **2017**, *9* (42), 37332−37339.
(26) Legge, C.; Davis, F.; Mitchell, G. Memory Effects in Liquid Crystal Elastomers. *J. Phys. B: At. Mol. Phys.* **1991**, *1* (10), 1253−1261.
(27) Spillmann, C. M.; Ratna, B. R.; Naciri, J. Anisotropic Actuation in Electroclinic Liquid Crystal Elastomers. *Appl. Phys. Lett.* **2007**, *90* (2), 021911.
(28) Kotikian, A.; Truby, R. L.; Boley, J. W.; White, T. J.; Lewis, J. A. 3D Printing of Liquid Crystal Elastomeric Actuators with Spatially Programed Nematic Order. *Adv. Mater.* **2018**, *30* (10), 1706164.
(29) Valenzuela, C.; Chen, Y.; Wang, L.; Feng, W. Functional Liquid Crystal Elastomers Based on Dynamic Covalent Chemistry. *Chem.−Eur. J.* **2022**, *28*, No. e202201957.
(30) Wang, Z.; Cai, S. Recent Progress in Dynamic Covalent Chemistries for Liquid Crystal Elastomers. *J. Mater. Chem. B* **2020**, *8*, 6610−6623.
(31) Pei, Z.; Yang, Y.; Chen, Q.; Terentjev, E. M.; Wei, Y.; Ji, Y. Mouldable Liquid-Crystalline Elastomer Actuators with Exchangeable Covalent Bonds. *Nat. Mater.* **2014**, *13* (1), 36−41.
(32) Lindberg, C. A.; Ghimire, E.; Chen, C.; Lee, S.; Dolinski, N. D.; Dennis, J. M.; Wang, S.; de Pablo, J. J.; Rowan, S. J. Exploring the Effect of Dynamic Bond Placement in Liquid Crystal Elastomers. *J. Polym. Sci.* **2023**, DOI: 10.1002/pol.20230547.
(33) Yang, Y.; Terentjev, E. M.; Wei, Y.; Ji, Y. Solvent-Assisted Programming of Flat Polymer Sheets into Reconfigurable and Self-Healing 3D Structures. *Nat. Commun.* **2018**, *9* (1), 1906.
(34) Tang, D.; Zhang, L.; Zhang, X.; Xu, L.; Li, K.; Zhang, A. Bio-Mimetic Actuators of a Photothermal-Responsive Vitrimer Liquid Crystal Elastomer with Robust, Self-Healing, Shape Memory, and Reconfigurable Properties. *ACS Appl. Mater. Interfaces* **2022**, *14* (1), 1929−1939.
(35) Wang, Z.; Tian, H.; He, Q.; Cai, S. Reprogrammable, Reprocessible, and Self-Healable Liquid Crystal Elastomer with Exchangeable Disulfide Bonds. *ACS Appl. Mater. Interfaces* **2017**, *9* (38), 33119−33128.
(36) Saed, M. O.; Terentjev, E. M. Catalytic Control of Plastic Flow in Siloxane-Based Liquid Crystalline Elastomer Networks. *ACS Macro Lett.* **2020**, *9* (5), 749−755.
(37) Saed, M. O.; Terentjev, E. M. Siloxane Crosslinks with Dynamic Bond Exchange Enable Shape Programming in Liquid-Crystalline Elastomers. *Sci. Rep.* **2020**, *10* (1), 6609.
(38) Denissen, W.; Winne, J. M.; Du Prez, F. E. Vitrimers: Permanent Organic Networks with Glass-like Fluidity. *Chem. Sci.* **2016**, *7* (1), 30−38.
(39) Saed, M. O.; Gablier, A.; Terentejv, E. M. Liquid Crystalline Vitrimers with Full or Partial Boronic-Ester Bond Exchange. *Adv. Funct. Mater.* **2020**, *30* (3), 1906458.
(40) Van Lijsebetten, F.; Debsharma, T.; Winne, J. M.; Du Prez, F. E. A Highly Dynamic Covalent Polymer Network without Creep: Mission Impossible? *Angew. Chem., Int. Ed.* **2022**, *61*, No. e202210405.
(41) Chen, Q.; Li, Y.; Yang, Y.; Xu, Y.; Qian, X.; Wei, Y.; Ji, Y. Durable Liquid-Crystalline Vitrimer Actuators. *Chem. Sci.* **2019**, *10* (10), 3025−3030.
(42) Wu, Y.; Yang, Y.; Qian, X.; Chen, Q.; Wei, Y.; Ji, Y. Liquid-Crystalline Soft Actuators with Switchable Thermal Reprogrammability. *Angew. Chem., Int. Ed.* **2020**, *59* (12), 4778−4784.
(43) Vozzolo, G.; Ximenis, M.; Mantione, D.; Fernández, M.; Sardon, H. Thermally Reversible Organocatalyst for the Accelerated Reprocessing of Dynamic Networks with Creep Resistance. *ACS Macro Lett.* **2023**, *12*, 1536−1542.
(44) Taplan, C.; Guerre, M.; Du Prez, F. E. Covalent Adaptable Networks Using β-Amino Esters as Thermally Reversible Building Blocks. *J. Am. Chem. Soc.* **2021**, *143* (24), 9140−9150.
(45) Lin, X.; Zou, W.; Terentjev, E. M. Double Networks of Liquid-Crystalline Elastomers with Enhanced Mechanical Strength. *Macromolecules* **2022**, *55* (3), 810−820.
(46) Lee, Y.; Choi, S.; Kang, B.-G.; Ahn, S.-k. Effect of Isomeric Amine Chain Extenders and Crosslink Density on the Properties of Liquid Crystal Elastomers. *Materials* **2020**, *13*, 3094.
(47) Yoon, H. H.; Kim, D. Y.; Jeong, K. U.; Ahn, S. K. Surface Aligned Main-Chain Liquid Crystalline Elastomers: Tailored Proper-

ties by the Choice of Amine Chain Extenders. *Macromolecules* **2018**, *51* (3), 1141−1149.
(48) Paramarta, A.; Webster, D. The Exploration of Michael-Addition Reaction Chemistry to Create High Performance, Ambient Cure Thermoset Coatings Based on Soybean Oil. *Prog. Org. Coat.* **2017**, *108*, 59−67.
(49) Peyrton, J.; Avérous, L. Aza-Michael Reaction as a Greener, Safer, and More Sustainable Approach to Biobased Polyurethane Thermosets. *ACS Sustain. Chem. Eng.* **2021**, *9* (13), 4872−4884.
(50) Ecochard, Y.; Auvergne, R.; Boutevin, B.; Caillol, S. Linseed Oil-Based Thermosets by Aza-Michael Polymerization. *Eur. J. Lipid Sci. Technol.* **2020**, *122*, 1900145.
(51) Thomas, C.; Peruch, F.; Deffieux, A.; Milet, A.; Desvergne, J. P.; Bibal, B. Phenols and Tertiary Amines: An Amazingly Simple Hydrogen-Bonding Organocatalytic System Promoting Ring Opening Polymerization. *Adv. Synth. Catal.* **2011**, *353* (7), 1049−1054.
(52) Wu, D.; Liu, Y.; He, C.; Chung, T.; Goh, S. Effects of Chemistries of Trifunctional Amines on Mechanisms of Michael Addition Polymerizations with Diacrylates. *Macromolecules* **2004**, *37* (18), 6763−6770.
(53) Merkel, D. R.; Shaha, R. K.; Yakacki, C. M.; Frick, C. P. Mechanical Energy Dissipation in Polydomain Nematic Liquid Crystal Elastomers in Response to Oscillating Loading. *Polymer* **2019**, *166*, 148−154.
(54) Sims, M. T.; Abbott, L. C.; Richardson, R. M.; Goodby, J. W.; Moore, J. N. Considerations in the Determination of Orientational Order Parameters from X-Ray Scattering Experiments. *Liq. Cryst.* **2019**, *46* (1), 11−24.

https://doi.org/10.1021/acs.macromol.3c02318
Macromolecules 2024, 57, 682−690